

Specific Energy Absorbed Study Of Aluminum (2024-351T) Tubes Alloy Under Lateral Crush

Ayad Arab Ghaidan

Lecturer

Civil Engineering Department, Kirkuk University

Abstract

This paper aims to find SEA (Specific Energy Absorber) for lateral crushing (statically) behavior for Aluminum (2024-T351) alloy with difference lengths (10, 20, and 30 mm). An experimental, finite element simulation, and theoretical models present to find force-deformation curves and then find SEA for difference lengths. Experimental results more agreements with finite elements simulation and theoretical when length of tubes is increase for load deformation curve, because when the length increases the plastic region increase with initial plastic collapse load (P_c). The experimental, ANSYS simulation and theoretical results have plotted and it has seen that the theory also underestimates the ANSYS results because in theoretical model, is customary to assume that the material is perfectly plastic, therefore, the finite element simulation might predict the experimental results better than the theoretical one. The results show that light density Aluminum alloy is suitable for SEA.

Keywords: SEA, Lateral crushing, Finite element method by Ansys.

دراسة امتصاص الطاقة النوعية لأنابيب الألمنيوم (2024-351T) تحت الأحمال الجانبية

الخلاصة

هدف هذا البحث هو إيجاد امتصاص الطاقة النوعية (SEA) لحمل جانبي على أنابيب سبيكة الألمنيوم (2024-T351) بأطوال مختلفة (10,20,30) ملم. تم المقارنة بين النتائج التي حصلت عليها عمليا مع نتائج المحاكاة و النتائج النظرية لمنحنيات القوة و الانبعاج و كذلك (SEA) و الانبعاج و لأطوال مختلفة، و تبين بأن النتائج العملية تتقارب مع نتائج المحاكاة و النتائج النظرية كلما زاد طول الأنابيب و ذلك بسبب كلما زاد طول الأنابيب تزداد معه منطقة اللدونة وكذلك حمل الانهيار لللدن الابتدائي (P_c). تم دراسة نتائج التي حصلت عليها عمليا و نتائج المحاكاة (ANAYS) و النتائج النظرية تبين بان النتائج النظرية تكون بعيدة عن نتائج المحاكاة و ذلك عند صياغة النموذج الرياضي (النظري) فُرضت بان النموذج (المادة) تكون بالكامل بلاستيك، ولكن نتائج المحاكاة تكون قريبة جدا إلى النتائج العملية أكثر منة إلى النتائج النظرية و أظهرت أيضا بان الكثافة القليلة للألمنيوم أفضل ل (SEA) .

الكلمات الدالة: SEA(امتصاص الطاقة النوعية)، السحق الجانبي، المحاكاة بواسطة انسس.

Notation

D: outer diameter of tubes
P: applied load
E: young modulus
 σ_u : ultimate strength
 ν : Poisson's ratio
G: shear modulus

SEA: specific energy absorbed

t: thickness

b: breath of the tubes

P_c : initial plastic collapse

Y: yield strength

M_p : plastic bending moment/ unit length

R: mean radius of tubes

Mp: plastic bending moment/ unit length

Introduction

The use of circular metallic tubes and rings in the design of crashworthy systems has attracted the attention of many researches. This area of research has been reviewed by Johnson and Reid^[1]. Circular sections are also widely used as cheap structural elements. Therefore, for better utilization of tubular structures, a thorough understanding of their collapse mechanism has been believed necessary. Thin metal tubes and rings can be arranged in different forms and loaded to deform in different modes to operate over a range of loads and stroke^[2]. The behavior of circular metal tubes under axial and lateral load has been studied by several researches. The tube under lateral (i.e. diametric or central) compression has some advantage over the axially loaded one and easier to build than most other devices^[3]. As a first step towards deciding the load-deflection characteristic of these structures under impact conditions, their behavior under quasistatic loading is usually examined. An examination of the relevant literature reveals that investigations have increasingly reported on the plastic deformation of tubular sections due to concentrated^{[4][5]} and^[6], and to locally and uniformly distributed lateral loads^[7]. Tube crushed between rigid plates shown in Figure (2) is the aim of this study. The subject has been searched by DE RUNTZ^[8]. by assuming rigid-perfectly plastic material. It has been reported that the theory underestimated the experimental results. Reid and Bell^[9] have been incorporated the influence of strain hardening. Even with the modification, a discrepancy exists between the results of theory and experiments. In an attempt to discover the remaining discrepancy, finite

element method, which can be used with confidence to simulate the complex response characteristic of structures, is employed. Design and analysis of the structural behavior of energy absorbers being integral parts of chassis frames is presented by Abramowicz W.^[10]. Methods of the analysis of the initial phase of failure and the estimation of an amount of the energy dissipated by the tubular absorber (single or multi-member) subject to lateral crushing load are presented^[11]. ANSYS/Mechanical (Version 11) finite element program package is used for the modeling the whole analysis of the gross deformation of even the simplest structure is most complicated. Therefore, usually simplifying assumptions, which lead to approximate expressions for the load-deflection relationship, are made. Especially, when bending mode predominates the deformation, it is customary to assume that the material is perfectly plastic and plastic hinges are formed at critical sections of the structure. The geometry of the structure is modified by assuming that the rigid portions undergo finite rotations about the plastic hinges and the load is allowed to increase beyond its collapse value. In the model, elastic-perfectly plastic material is assumed and SOLID45 (8-nodes bricks) elements are used. The predictions are compared with the theoretical and experimental results and an agreement is seen.

To compare different materials or forms in their ability of energy absorption, the SEA (Specific Energy Absorbed) ratio expressed in equation (10) was used for this study. It divides the work that is done on the object by the product of its volume and the density of the material. This SEA is supposed to be as high as possible for an optimal benefit. Several applications like the former mentioned racing sport demand low weight.

Especially in those cases a high SEA is necessary to fulfill the need of optimal energy absorption and savings in weight at the same time. The target behavior of the deformation process in the case of an impact is a constant absorption curve. The energy should be absorbed in a controlled manner. Lateral crushed tubes show this kind of behavior

Theory

The whole analysis of the gross deformation of even the simplest structure is most complicated. Therefore, usually simplifying assumptions, which lead to approximate expressions for the load-deflection relationship, are made. Especially, when bending mode predominates the deformation, it is customary to assume that the material is perfectly plastic and plastic hinges are formed at critical sections of the structure. The geometry of the structure is modified by assuming that the rigid portions undergo finite rotations about the plastic hinges and the load is allowed to increase beyond its collapse value.

A thin circular tube is not too flexible, of mean radius R when subjected to diameter load P can only collapse plastically when four hinges have been formed to permit it to behave as a mechanism, see Figure (1). The plastic hinges are assumed to arise at the locations where maximum elastic occur. If the center of the tube, O , remains stationary, then at collapse the four rigid portions of the tube between the hinges rotate with angular speed, Ω , about instantaneous center, I , and the force P , move towards the center of the tube with speed $R \cdot \Omega$. The work input rate therefore $2PR \Omega$ and the plastic work dissipation rate is $8M_p \Omega$. Thus,

$$2P \cdot R\Omega = 8M_p \cdot \Omega$$

And hence

$$P = 4M_p/R \dots\dots\dots (1)$$

When continued quasi-static crushing of a tube occurs between rigid, parallel surface, it is evident that the crushing force increases with reduction in vertical diameter of the ring. An indication of the force – vertical deflection characteristic to be expected is to be had by conceiving the deformation to proceed as indicated in Figure (2). The original four plastic hinges are maintained but the points of application of the compressing forces move away the centre line, splitting in to two equal components, $P/2$. Each quadrant of the ring may be supposed to rotate though remaining rigid. Applying the same work approach as above, for one quadrant, we have.

$$\frac{P}{2} NI \cdot \Omega = 2M_p \cdot \Omega$$

$$P = \frac{4M_p}{NI} \dots\dots\dots (2)$$

Fully plastic bending moment per unit length of the ring, M_p is given by

$$M_p = \frac{Yt^2}{4} \dots\dots\dots (3)$$

Where Y and t denoted the uniaxial yield strength of the tube material and thickness of the ring, respectively, so the initial plastic collapse load, P_c is equal to

$$P_c = \frac{4M_p b}{R} \dots\dots\dots (4)$$

Where R is the mean radius equal to (D-t), where D is the outer diameter and b is the breadth of the tube.

If δ denotes the total tube deformation $NI^2 = (D^2 - \delta^2)$ and thus

$$\frac{P}{4M_{p/R}} = \frac{1}{[1 - (\delta/D)^2]^{1/2}} \dots\dots\dots(5)$$

Where P is the post – collapse load, and thus

$$P = \frac{4M_{p/R}}{[1 - (\delta/D)^2]^{1/2}} \dots\dots\dots(6)$$

Above equation is the expression the collapse load per unit length, so the collapse load can be written

$$P = \frac{4M_p b/R}{[1 - (\delta/D)^2]^{1/2}} \dots\dots\dots(7)$$

So,

$$P = \frac{P_c}{[1 - (\delta/D)^2]^{1/2}} \dots\dots\dots(8)$$

The form of this P/δ curve is shown in fig (2) for difference length (10, 20, and 30) mm; this solution holds for $0 \leq \beta \leq \pi/4$. A frictional force of $\mu P/2$ would modify, where μ is coefficient of friction equal to 0.61.

$$P = \frac{P_c}{[1 - (\delta/D)^2]^{1/2} + \mu(1 - \cos\beta)} \dots\dots(9)$$

Experimental Work

Round tubes of Aluminum (2024-T351) of different sizes were subjected to load of 10 ton statically lateral compression

in a machine is shown in figure (3). Tubes have been crushed between two rigid flat plates (top and bottom flat plates), for the bottom plat is fixed. The upper plat is supposed to move in negative y-direction. The speed of testing was generally at 2mm/min, and load-compression curves in the tests were recorder. Round tubes employed in these tests were of three different sizes. The mean diameter (D_m) of the tubes equal to 28mm and wall thickness was kept at t=2mm. the length of the tubes varied (10, 20, 30) mm. the chemical compositions and mechanical properties for (2024-T351) Al. Alloy are shown in tables (1) and (2) respectively. When the load applied in the specimen the deformation occur and diameter decreased figures (4) is shown the deformation procedure. The relationship between load and deformation under lateral compression for length (10, 20, and 30) mm are shown in Figures (5), (6), and (7) respectively. Matlab program is used to curve fitting for experimental data's .To compare material with different length in their ability of energy absorption, the (SEA) Specific energy absorbed ratio Expressed in equation below was used for this study. It divided the work that is done on the object by the product of its volume (v), and density of material(ρ), where work down (W) equal to product of applied load (P) and deformation(δ) of the tubes so, work done equal to P.δ can be obtained from p- δ curves.

$$SEA = \frac{W}{V\rho} \dots\dots\dots(10)$$

Where: W is Work done, V is the volume, and ρ is the density equal to ($2.7 \cdot 10^3 \text{Kg/m}^3$) for (2024-T351) Al. alloy.

The relationship between (SEA) and deformation (δ) experimentally for different lengths are shown in Figure (8), the relationship between (SEA) and length experimentally is shown in Fig. (10) with different deformation (δ) in diameters.

Finite Element Simulation

Finite element simulation was performed on time is Approximately 50 min. The modeling consists of the following phases.

Model Discretization

A mapped mesh consisting of brick elements (ANSYS element type SOLID45) are used for the three-dimensional modeling of solid structures Figure (12). Eight nodes having three degrees of freedom at each node define the element: translations in the nodal x, y, and z directions. The element has plasticity, stress stiffening, large deflection, and large strain capabilities. Cross-sectional dimensions are (10, 20, 30) mm and 2 mm corresponds to breadth and thickness of a tube. Number of element divisions along the breadth and thickness are (3, 5, 9) and 1, are shown in Figure (12) respectively. 4320 SOLID45 elements are positioned on a tube with an outside diameter 30 mm.

Material Properties

For the modeling as received Aluminum (2024-T351) has been chosen since it has been observed that, under simple tension test, as received Aluminum behaves nearly as an elastic-perfectly plastic material Figure (13). Yield strength of the material was measured as 344 MPa from a simple tension test. In the modeling elastic modulus and Poisson's ratio were taken as 71 GPa and 0.3, respectively.

Boundary Conditions

We use the "Rigid" material to define the boundary conditions because the tubes

are crashed between two rigid flat materials. The "Rigid" material offers the option to define rotational and translational boundary conditions for all parts that are meshed with the material "Rigid". Because we created two material models using the "Rigid" material (bottom and upper) we can easily define different boundary conditions for the two parts. For the bottom material, we prohibit displacement in all translational directions and around every rotational axis. The upper material is supposed to move in negative y-direction.

Loading History

One-step displacement, which is 22 mm radial compression, is given to the rigid flat material at the top of the ring. Deformed mesh is shown in Figures (16, and 17) for lengths (10, and 30) respectively, which shows the deformation distribution. Loads deformation curves for one nod are shown in Figures (14, and 15).

Discussion and Conclusions

Load–deformation for theoretical, experimental with MATLAB polynomial, and finite elements models simulations are given in Figure (5, 6, &7) showed a good agreement. Experimental results more agreements with finite elements simulation and theoretical when length of tubes is increase for load deformation curve, because when the length increases the plastic region increase with initial plastic collapse load (P_c).

SEA-length experimental curves have given in Figure (8) for different lengths. It compares with finite element and theoretical results have shown in figure (10). SEA increases when size of tubes decrease, Figure (9) shows the SEA for different lengths at 2mm deformation. SEA are much closed to each other, but when the length is less than 20mm SEA-

length curves are incline curves. The curves became much incline when deformation increases. When the length is greater than 20 mm the SEA-lengths became horizontal line with progress length. The comparison between the experimental results and finite element results has given in figure (11). This figure gives a good agreement of SEA and length relationship for different lengths.

As received Aluminum behaves as a rigid-perfectly plastic material as shown from stress strain curve. Therefore, the theory must fit the experimental result. However, it was seen from the previous papers that the theory underestimates the experimental result. The experimental and theoretical, ANSYS results have plotted and it has seen that the theory also underestimates the ANSYS results. Therefore, the finite element simulation might predict the experimental results better than the theoretical one. Although the obtained deviations are within the acceptable limits, including the strain hardening and strain rate effects can modify material properties in ANSYS model. These modifications, which remain to be investigated, will certainly result in more results that are realistic.

References

- 1- Johnson, W. and Reid, S. R., "Metallic Energy Dissipating Systems", (1978).
- 2- Appl. Mech. Revs., Vol. 31, pp 277-288.
- 3- Reid, S. R., and Reddy, T. Y. "Inelastic Behaviour of Plates and Shells", IUTAM Symp., Rio de Janeiro, Springer, Berlin, (1986).
- 4- Reddy, T. Y. and Reid, S. R., "Lateral Compression of Tubes and Tube-Systems with Side Constraints", Int. J. Mech. Sci., Vol. 21, pp 187-199, (1979).
- 5- Deruntz, J. A. and Hodge, P. G., "Crushing of a Tube Between Rigid Plates", J. Appl. Mech., Vol. 30, pp 391-394, (1963).
- 6- Reid, S. R. and Reddy, T. Y. "Effect of Strain Hardening on the Lateral Compression of Tubes Between Rigid Plates", Int. J. Solids Structures, Vol. 14, pp213-225, (1978).
- 7- Reddy, T. Y. and Reid, S. R. "On Obtaining Material Properties from the Ring Compression Test", Nuclear Engng Design, Vol. 52, pp. 257-263, (1979).
- 8- Johnson, W., Ghosh, S. K., Mamalis, A. G., Reddy, T. Y. and Reid, S. R., ("The Quasi-Static Piercing of Cylindrical Tubes or Shells", Int. J. Mech.Sci., Vol. 22, pp 9-20), (1980).
- 9- DE. Runtz, J. A and HODGE, P. G. "Crushing of a tube between rigid plates", J. appl. Mech., 391, (1963).
- 10- Reid, S. R. and Bell, W. W. "Influence of Strain Hardening on the Deformation of Thin Rings Subjected to Opposed Concentrated Loads", Int. J. Solids Structures, Vol. 18, pp 643-658, (1982).
- 11- Herakovich Carl T., "Mechanics of Fibrous Composites," Wiley, 1998.
- 12- Zeng Tao, "Dynamic crashing and impact energy absorption of 3D braided composite tubes," Elsevier, 2005.
- 13- Du Qyesnay D.L., Topper, T.H. and Yu.M.Y. "The effect of Notch radius on the fatigue Notch factor and propagation of short cracks". The behavior of short fatigue crakes. EGF, London.

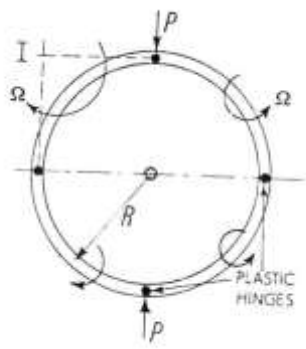


Figure (1) plastic hinges

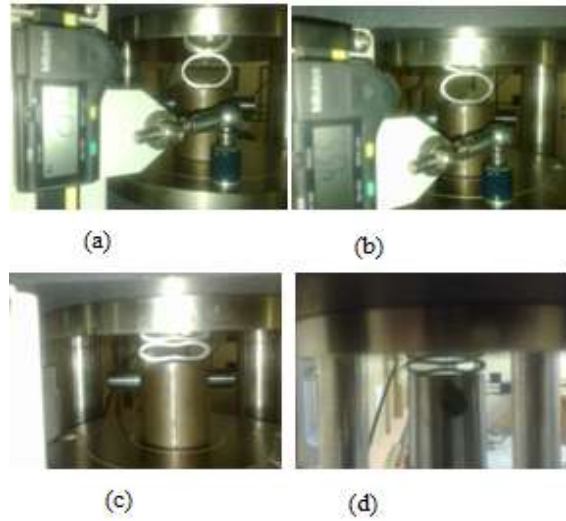


Figure (4) deformation procedure.

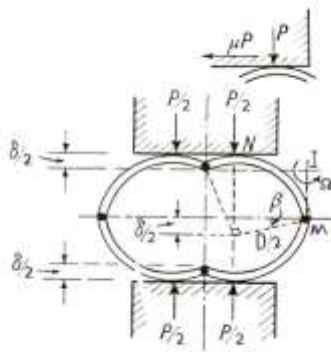


Figure (2) deformation procedure

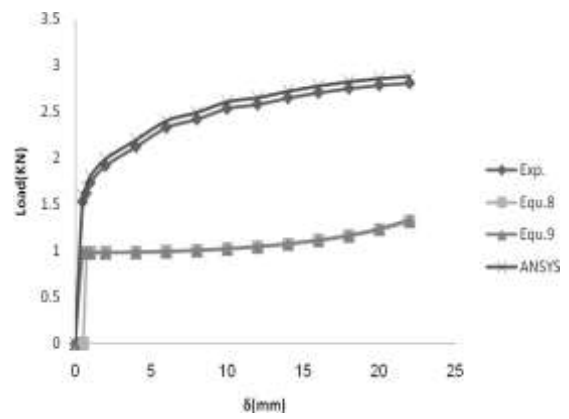


Figure (5) load (P) vs. deformation (δ), $b=10\text{mm}$



Figure (3) specimen under loads

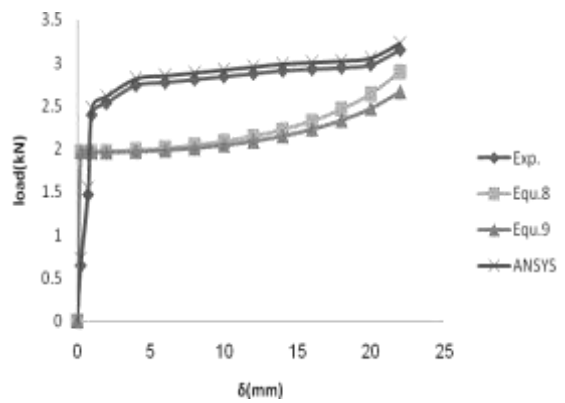


Figure (6) load (P) vs. deformation (δ), $b=20\text{mm}$

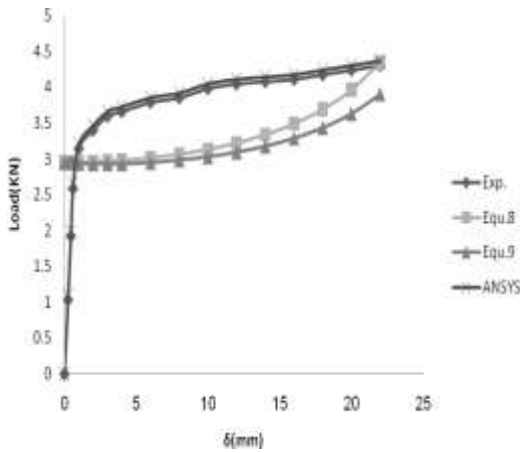


Figure (7) load (P) vs. deformation (δ), $b=30\text{mm}$

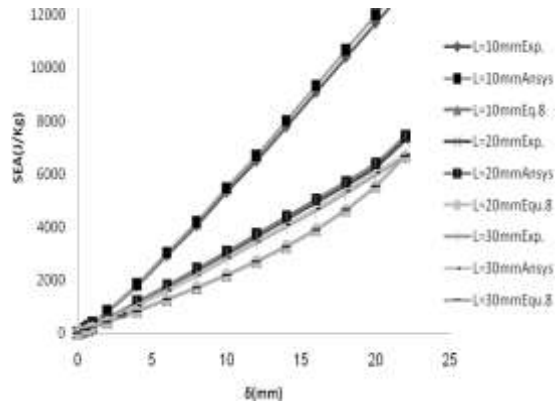


Figure (10) SEA vs tube length

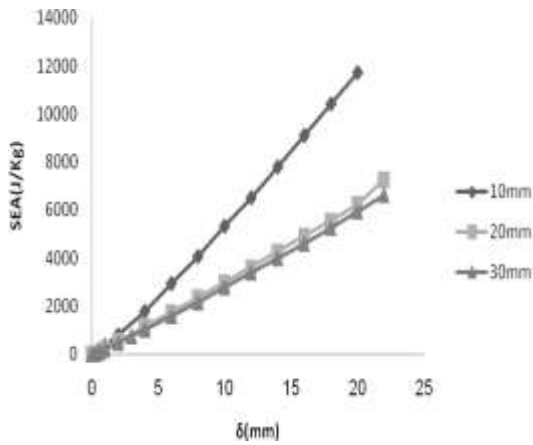


Figure (8) SEA vs. deformation (δ) for different length (10, 20, and 30) mm

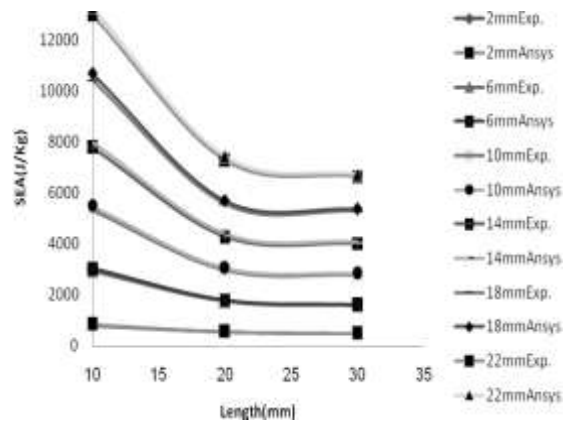


Figure (11) SEA vs. Tubes Length at different

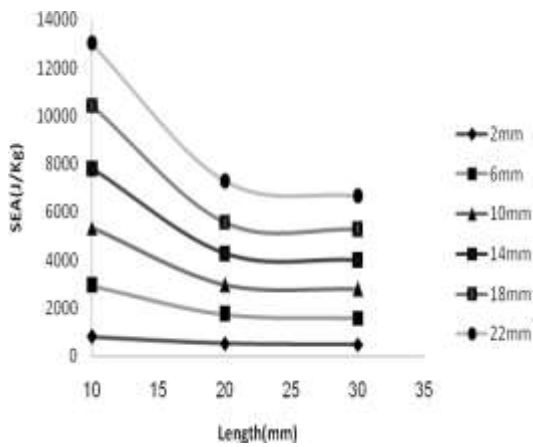


Figure (9) SEA vs. tube lengths (b) at different deformations

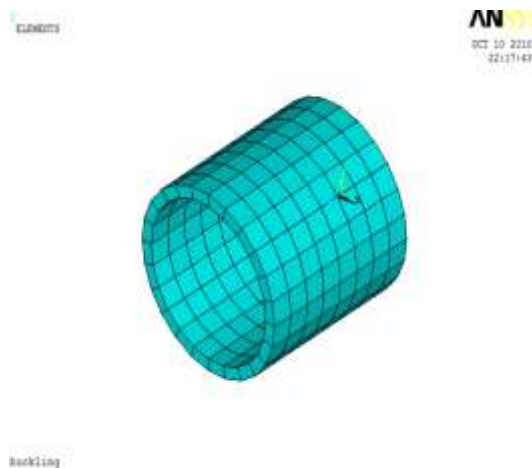


Figure (12) Ansys modal

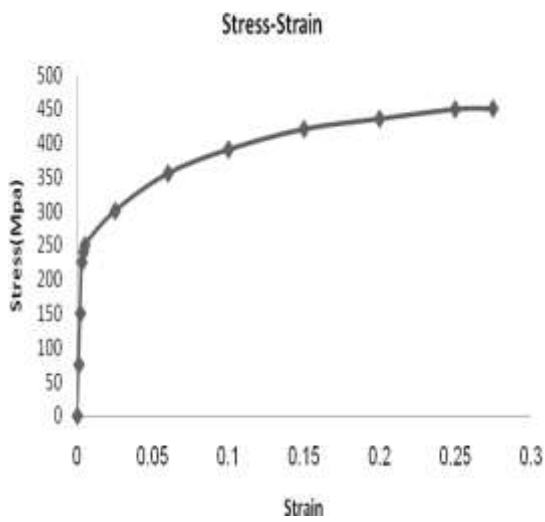


Figure (13) stress, strain diagram for Al Alloy.



Figure (16) deformation element tube b=10mm

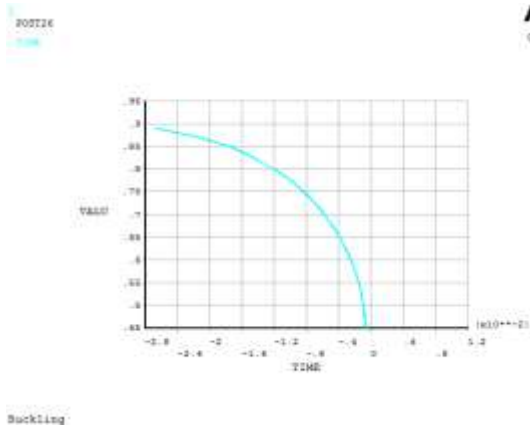


Figure (17) deformation elements tube b=30mm

Figure (14) load (N) vs. Deformation (mm) for one nod b=10mm

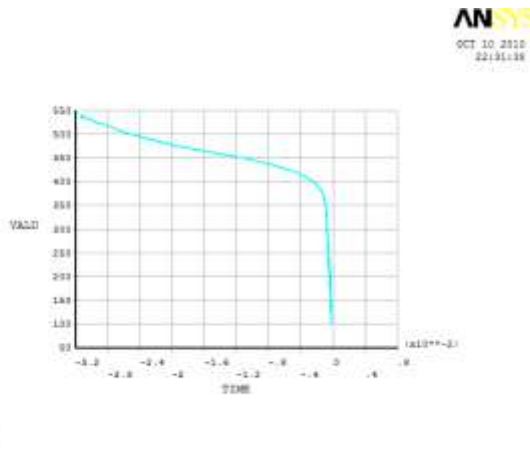


Figure (15) Load (N) vs. deformation (mm) for one nod b=30 mm

Table (1) chemical composition of 2024-T351 Al. alloy (wt %)

element	Si	Fe	Cu	Mg	Mn	Cr	Zn	Ti	Al
Exper.	0.51	0.5	4.37	1.44	0.7	0.1	0.25	0.15	Re m.
standard	0.5	0.5	3.8-4.9	1.2-1.8	0.3-0.9	0.1	0.25	0.15	Re m.
Ref. ^[12]	0.5	0.5	4.35	1.5	0.6	0.1	0.25	0.15	Re m.

Table (2) Mechanical properties of 2024-T351 Al. alloy.

symbols	Y(MPa)	σ_u (MPa)	E (GPa)	ν	G(GPa)
Exp.	344	457	71	0.3	27.5
standard	340-360	450-470	70-75	0.28	27-29
Ref. ^[12]	356	466.1	72.4	0.28	28

